

Production of H^+ fragments from H_2 by fast projectiles

A. K. Edwards, R. M. Wood, and M. F. Steuer

Department of Physics and Astronomy, University of Georgia, Athens, Georgia 30602

(Received 14 April 1977)

The yield of H^+ fragments from H_2 by fast beams (0.5–4 MeV) of H^+ , H_2^+ , He^+ , and O^+ is measured as a function of projectile velocity. The yields of H^+ from both the dissociative states of H_2^+ and from the double ionization of H_2 are identified. The H_2^+ projectile is comparable to He^+ in producing H^+ fragments from the single ionization of the H_2 target, but unlike He^+ it produces no appreciable double ionization.

INTRODUCTION

The cross section for ionization of H_2 by fast projectiles has been measured and compared to the Born approximation.¹⁻⁴ These measurements included the projectiles H^+ , He^+ , and He^{2+} in the energy range of 0.13–1 MeV, and were performed by collecting all positive charges produced from H_2 by the projectiles. The H_2^+ ions were collected along with the H^+ ions formed from dissociative ionization. These processes were not separated and treated individually. Using lower energy projectiles (5–50 keV) Afrosimov *et al.*⁵ measured each ionizing process produced by H^+ projectiles along with the final charge state of the projectile.

This article reports measurements of the yields of H^+ ions from the dissociative states of H_2^+ and from doubly ionized H_2 produced by fast projectiles passing through an H_2 target gas. The dissociative processes leading to the formation of H^+ are

separated as described previously,⁶ and the yield from each process is analyzed. The projectiles are H^+ , H_2^+ , He^+ , and O^+ in the energy range 0.5–4 MeV.

EXPERIMENTAL PROCEDURE

The experimental procedure is described in detail elsewhere,⁷ and only a brief discussion is given here. A pulsed beam of projectiles is focused into a chamber containing a static-gas H_2 target. The H^+ fragments emitted at 90° with respect to the beam direction pass through a parallel-plate energy analyzer to a channeltron detector. The pulsed beam allows measurement of the time of flight (TOF) of the fragment, and the analyzer allows measurement of its kinetic energy. This technique of measuring both TOF and energy separates the H^+ fragments from the H_2^+ ions and the contaminant ions O^+ and N^+ . The kinetic energy spectra of H^+ which are obtained are shown in Figs. 1–3.

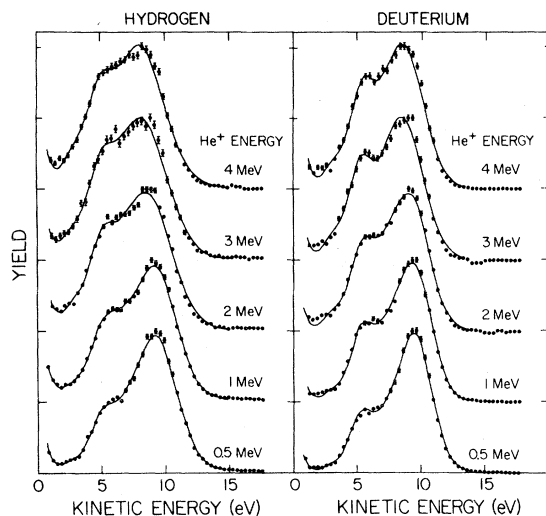


FIG. 1. H^+ and D^+ yields as a function of kinetic energy for 0.5- to 4-MeV He^+ incident on H_2 and D_2 . The spectra are normalized to the same height, and the error flags indicate purely statistical uncertainties. The solid curves are calculated fits to the data.

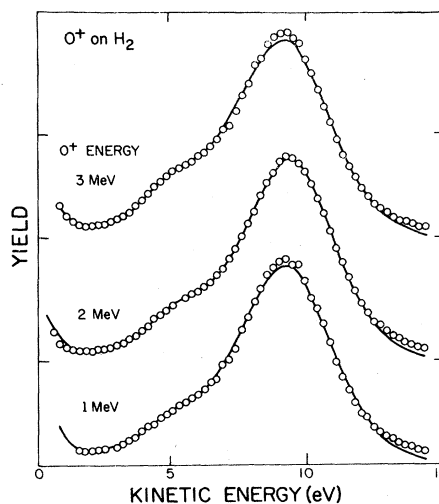


FIG. 2. H^+ yields as a function of kinetic energy for 1–3-MeV O^+ incident on H_2 . The spectra are normalized to the same height, and the error flags indicate purely statistical uncertainties. The solid curves are calculated fits to the data.

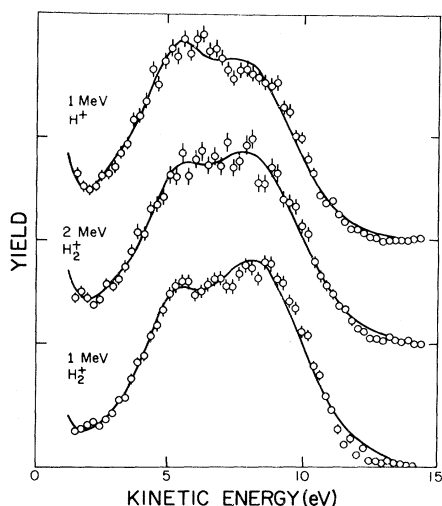


FIG. 3. H^+ yields as a function of kinetic energy for 1- and 2-MeV H_2^+ and 1-MeV H^+ incident on H_2 . The spectra are normalized to the same height, and the error flags indicate purely statistical uncertainties. The solid curves are calculated fits to the data.

The fast ion beam is collected in a Faraday cup, and the amount of charge collected during a run is measured. The pressure of the H_2 target gas is typically $\frac{1}{2}$ mTorr, which satisfies the condition for single collisions. The number of H^+ fragments detected is normalized to the beam particle flux and the target gas density. This normalized count is referred to as the yield of H^+ from the H_2 target. It should be emphasized that this yield is measured at 90° from the beam direction and does not represent a sum over all angles.

DATA REDUCTION

The reflection approximation⁸ is used to predict the spectra of H^+ from the dissociative states of H_2^+ and from doubly ionized H_2 . In this approximation, the relative intensity of the H^+ fragments as a function of dissociation energy is assumed proportional to the overlap integral between the H_2 ground state and the dissociative state. The overlap integral is calculated by assuming a δ -function relation for the dissociative state and an harmonic oscillator wave function for the ground state. These predicted spectra are in turn fitted to the data by a least-squares fitting program to determine the contribution of each to the measured spectrum. A more detailed discussion of this procedure is given elsewhere.⁶ The states included in the fitting routine are $1s\sigma_g$, $2p\sigma_u$, $2p\pi_u$, $2s\sigma_g$, H^+H^+ , and an assumed autoionizing state.⁶ The smooth curves drawn through the data shown in Figs. 1–3 are a result of the fitting procedure. Since both H_2 and D_2 results are very similar, only

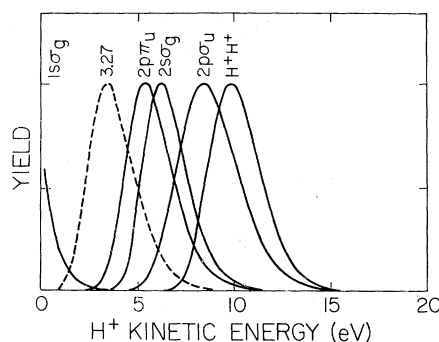


FIG. 4. Reflection approximation predictions of the shapes of the energy spectra produced by excitation and subsequent dissociation of the dissociative states of H_2^+ . The dashed curve is the prediction of the energy spectrum from an autoionizing state of H_2 and more details are given in Ref. 6.

H_2 is discussed further.

The spectra predicted by the reflection approximation are shown in Fig. 4 and are normalized to the same height. The curve labeled 3.27 is for a predicted autoionizing state and is needed to properly fit the data.⁶ The total yield represented by each curve of Fig. 4 is found by dividing the energy scale into small intervals or channels of width W_s and then summing the yields for each channel, viz., $\sum_J N_I(J)$ where I denotes one of the six curves of Fig. 4 and $N_I(J)$ is the yield in the J th channel for the I th curve. The area under the I th curve is then given by $\sum_J N_I(J)W_s$. The contribution of each of the six states to the yield recorded in a measured spectrum (Figs. 1–3) is given by a coefficient A_I such that

$$\sum_J Y(J)W_D = \sum_I A_I \sum_J N_I(J)W_s,$$

where $\sum_J Y(J)$ is a summation of the measured yields in each channel and W_D is the energy interval of each channel used in data collection. The A_I 's are determined from the fitting routine mentioned above. The fraction of the total measured yield for a given projectile and projectile energy that is produced from the I th dissociative state is then given by

$$F_I = \frac{W_s}{W_D} \frac{A_I \sum_J N_I(J)}{\sum_J Y(J)},$$

and that part of the total measured yield that comes from the I th dissociative state is given by

$$Y_I = F_I \sum_J Y(J).$$

For H^+ fragment energies below 1.5 eV, the energy distributions may be distorted by surface ef-

fects, so only channels corresponding to energies greater than 2 eV were included in the calculations.⁹

RESULTS

The yield of H⁺ fragment ions from the breakup of H₂ by the different projectiles is separated into three groups: the yield resulting from the dissociative states $2p\sigma_u$ and $2p\pi_u$ of H₂⁺; the yield produced by the double ionization of H₂; and that resulting from the $1s\sigma_g$, $2s\sigma_g$, and 3.27 states. These last three states included in the analysis contribute only slightly⁶ to the production of H⁺ with energies above 2 eV. The functional dependence of the H⁺ yield on beam velocity is nearly identical for the $2p\sigma_u$ and $2p\pi_u$ states, so the yields from these states are summed. The H⁺ yield from double ionization shows a different beam-velocity dependence than do the H₂⁺ dissociative states.

The yield of H⁺ from the $2p\sigma_u$ and $2p\pi_u$ states of H₂⁺ as a function of projectile velocity is shown in Fig. 5. The $2p\sigma_u$ contributes about 65% of the yield.⁶ The smooth line in Fig. 5 is calculated from the Bethe-Born approximation¹⁰ and has the form

$$Y = A \frac{\ln[B(E/M)]}{E/M}$$

where E is the projectile energy and M is the projectile mass. The value of B is taken from the proton ionization measurements of Hooper *et al.*,² and A is found from normalizing to the He⁺ data point at 2 MeV which corresponds to a projectile velocity of $0.707 \text{ (MeV/amu)}^{1/2}$. The shape of the

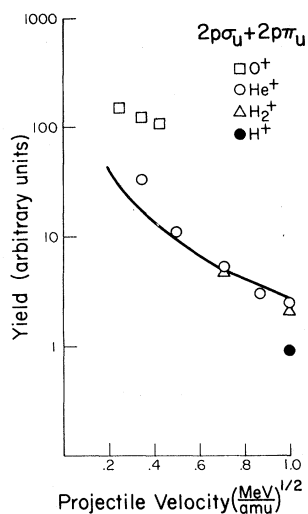


FIG. 5. Yield of H⁺ from the $2p\sigma_u$ and $2p\pi_u$ states of H₂⁺ as a function of projectile velocity.

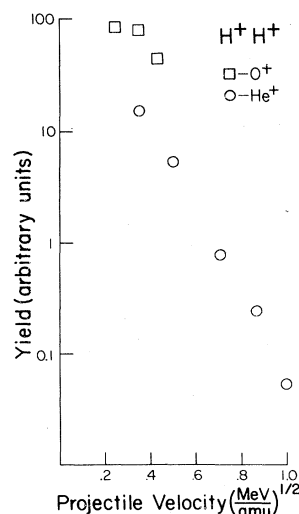


FIG. 6. Yield of H⁺ from the double ionization of H₂ as a function of projectile velocity.

curve does not depend critically on the value of B .

Figure 6 shows the yield of H⁺ from the double ionization of H₂. Only the He⁺ and O⁺ projectiles produce any appreciable double ionization. The He⁺ measurements are seen to decrease exponentially with beam velocity. For single ionization of H₂, it is shown in Fig. 5 for two different beam velocities that H₂⁺ and He⁺ projectiles are comparable. However, H₂⁺ produces practically no double ionization at these velocities. The same is true of the H⁺ beam. The total yield of H⁺ fragments from the dissociative states of H₂⁺ and from double ionization is shown in Fig. 7.

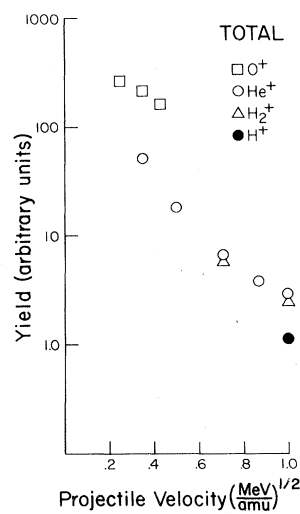


FIG. 7. Total normalized yield of H⁺ as a function of projectile velocity.

TABLE I. Fractions of the total H^+ yield above 2 eV due to excitation of the states indicated in the second column.

Beam	State	Bombarding energy (MeV)					Uncertainty
		0.5	1	2	3	4	
He^+	3.27	0.06	0.07	0.11	0.12	0.10	± 0.02
	$2s\sigma_g$	0.01	0.08	0.03	0.05	0.02	0.03
	$2p\pi_u$	0.22	0.20	0.28	0.28	0.31	0.02
	$2p\sigma_u$	0.43	0.36	0.48	0.51	0.54	0.06
	H^+H^+	0.29	0.29	0.12	0.06	0.02	0.06
O^+	3.27		0.05	0.05	0.06		± 0.02
	$2s\sigma_g$		0	0.01	0		0.03
	$2p\pi_u$		0.13	0.14	0.17		0.02
	$2p\sigma_u$		0.44	0.43	0.50		0.06
	H^+H^+		0.32	0.37	0.27		0.06
H_2^+	3.27		0.12	0.14			± 0.02
	$2s\sigma_g$		0	0.05			0.03
	$2p\pi_u$		0.34	0.32			0.02
	$2p\sigma_u$		0.55	0.49			0.06
	H^+H^+		0	0			0.06
H^+	3.27		0.20				± 0.02
	$2s\sigma_g$		0.05				0.03
	$2p\pi_u$		0.37				0.02
	$2p\sigma_u$		0.44				0.06
	H^+H^+		0				0.06

Table I lists the fractions of the total yield of H^+ fragments from dissociative ionization of H_2 with energy greater than 2 eV. Table II lists the fraction of the yield from the states which dissociate to $H+H^+$. This yield has been referred to previously⁶ as the reduced yield, and it is the total yield minus the yield due to double ionization.

The fractions of the reduced yield are found to be independent of the projectile velocities, and the average of the measurements at different beam energies are listed. However, the presumed 3.27 autoionizing state does show a slight monotonic increase with projectile energy.

TABLE II. Fraction of the reduced yield due to excitation and dissociation of the states listed. The reduced yield is the total yield minus the yield due to double ionization. These reduced fractions are averages of the measurements at different beam energies.

Beam \ State	$2p\sigma_u$	$2p\pi_u$	$2s\sigma_g$	3.27
O^+	0.67 ± 0.15	0.21 ± 0.05	0.01 ± 0.05	0.07 ± 0.04
H_2^+	0.52 ± 0.09	0.33 ± 0.04	0.02 ± 0.03	0.13 ± 0.03
He^+	0.55 ± 0.09	0.30 ± 0.04	0.05 ± 0.03	0.12 ± 0.03
H^+	0.44 ± 0.09	0.37 ± 0.04	0.05 ± 0.03	0.20 ± 0.03

- ¹J. W. Hooper, E. W. McDaniel, D. W. Martin, and D. S. Harmer, *Phys. Rev.* 121, 1123 (1961).
- ²J. W. Hooper, D. S. Harmer, D. W. Martin, and E. W. McDaniel, *Phys. Rev.* 125, 2000 (1962).
- ³R. A. Langley, D. W. Martin, D. S. Harmer, J. W. Hooper, and E. W. McDaniel, *Phys. Rev.* 136, A379 (1964).
- ⁴D. W. Martin, R. A. Langley, D. S. Harmer, J. W. Hooper, and E. W. McDaniel, *Phys. Rev.* 136, A385 (1964).
- ⁵V. V. Afrosimov, G. A. Leiko, Yu. A. Mamaev, and M. N. Panov, *Zh. Eksp. Teor. Fiz.* [Sov. Phys. JETP 29, 648 (1969)].
- ⁶R. M. Wood, A. K. Edwards, and M. F. Steuer, *Phys. Rev. A* 15, 1433 (1977).
- ⁷R. M. Wood, A. K. Edwards, and M. F. Steuer, *Rev. Sci. Instrum.* 47, 1471 (1976).
- ⁸A. S. Coolidge, H. M. James, and R. D. Present, *J. Chem. Phys.* 4, 193 (1936).
- ⁹M. F. Steuer, R. M. Wood, and A. K. Edwards, *Phys. Rev. A* (to be published).
- ¹⁰N. F. Mott and H. S. W. Massey, *The Theory of Atomic Collisions* (Clarendon, Oxford, 1964), p. 613.